

Magnetic relaxation in cobalt(II)-based single-ion magnets influenced by distortion of the pseudotetrahedral [N₂O₂] coordination environment

Michael Böhme, Sven Ziegenbalg, Azar Aliabadi, Alexander Schnegg, Helmar Görls,
Winfried Plass*

Electronic Supplementary Information (ESI)

Table S1: Crystallographic data and structure refinement parameters for **1** and **2**

	1	2
formula	C ₃₈ H ₂₈ CoN ₂ O ₂	C ₄₆ H ₃₂ CoN ₂ O ₂
formula weight (g mol ⁻¹)	603.55	703.67
crystal size (mm)	0.088 × 0.082 × 0.080	0.044 × 0.042 × 0.038
crystal system	orthorhombic	monoclinic
space group	<i>Pbcn</i>	<i>C2/c</i>
<i>a</i> (pm)	2021.52(4)	2534.89(7)
<i>b</i> (pm)	895.92(2)	881.26(2)
<i>c</i> (pm)	1583.27(3)	1602.15(3)
α (°)	90	90
β (°)	90	106.217(1)
γ (°)	90	90
<i>V</i> (10 ⁶ pm ³)	2867.49(10)	3436.63(14)
<i>Z</i>	4	4
<i>T</i> (K)	133(2)	133(2)
δ_{calc} (g cm ⁻³)	1.398	1.360
<i>F</i> (000)	1252	1460
μ (Mo K _α) (mm ⁻¹)	0.637	0.543
Θ range of data collection (°)	2.49 ≤ Θ ≤ 27.48	2.46 ≤ Θ ≤ 27.45
measured reflections	19230	11933
unique reflections (<i>R</i> _{int})	3290 (0.0713)	3903 (0.0243)
no. of parameters	251	295
goodness-of-fit on <i>F</i> ²	1.104	1.078
<i>R</i> 1 (<i>I</i> > 2σ(<i>I</i>))	0.0549	0.0303
<i>wR</i> 2 (all data)	0.1328	0.0705

Table S2: Comparison of the literature known and the obtained crystal structures of **2**

	Literature [S1]	2
space group	$C2/c$	$C2/c$
	<i>cell</i>	
a (pm)	2538.08(13)	2534.89(7)
b (pm)	883.92(4)	881.26(2)
c (pm)	1626.56(10)	1602.15(3)
α ($^{\circ}$)	90	90
β ($^{\circ}$)	105.756(6)	106.217(1)
γ ($^{\circ}$)	90	90
T (K)	293	133
	<i>Shape</i>	
$S(T_d)$	4.927	4.801
$S(D_{4h})$	15.454	15.676
δ ($^{\circ}$)	64.8	65.3

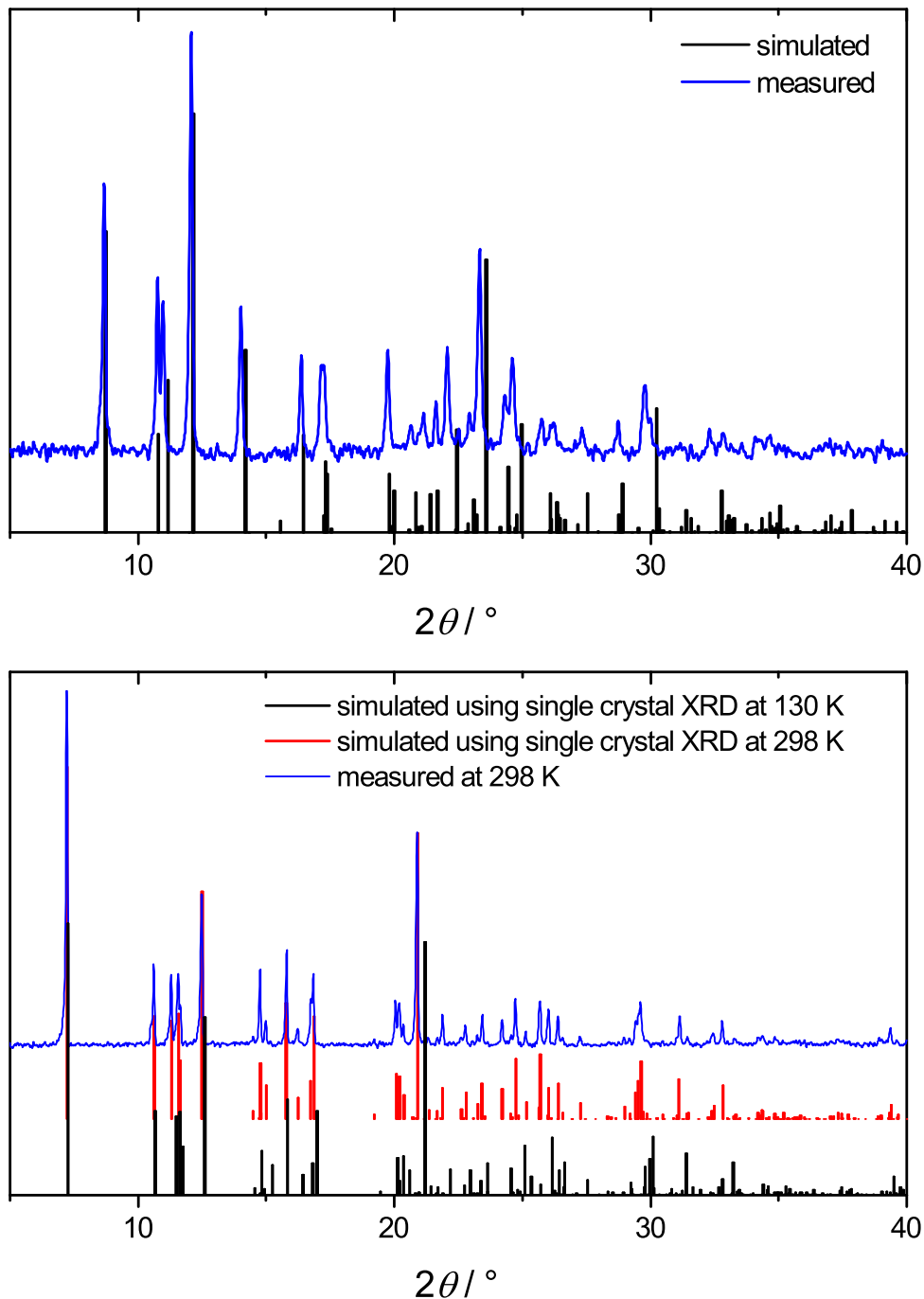


Fig. S1: X-ray powder diffraction (XRPD) patterns of **1** (top) and **2** (bottom) both measured at 298 K.

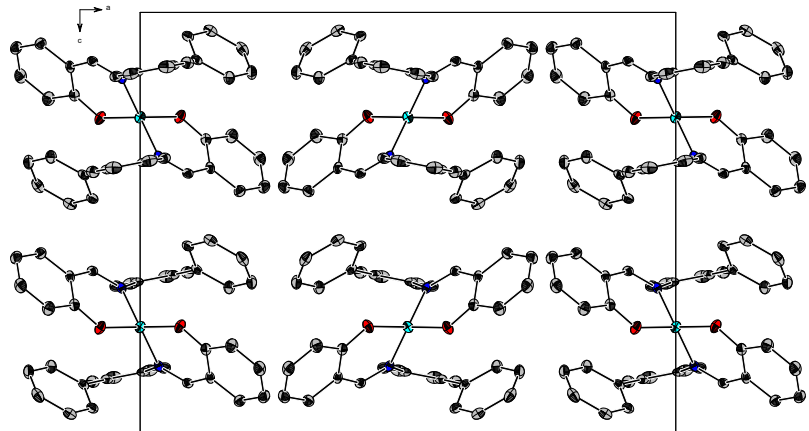


Fig. S2: Packing diagram for **1**, for clarity the intramolecular $\pi \cdots \pi$ interactions depicted in Fig. 1 are omitted here.

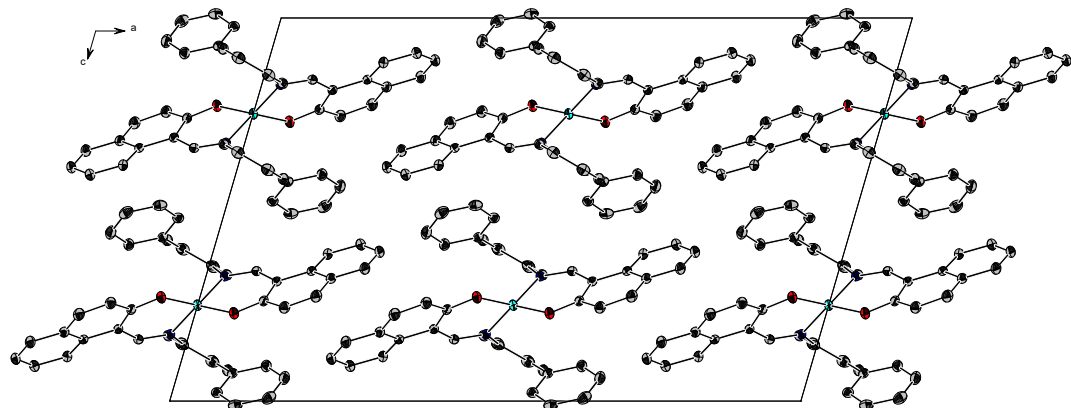


Fig. S3: Packing diagram for **2**, for clarity the intramolecular $\pi \cdots \pi$ interactions depicted in Fig. 1 are omitted here.

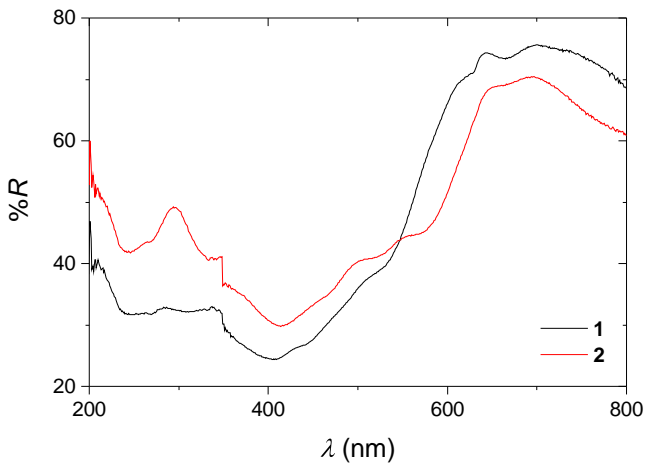


Fig. S4: Diffuse reflectance spectra of the compounds **1** and **2**. Note that a change of the light source occurs at 350 nm.

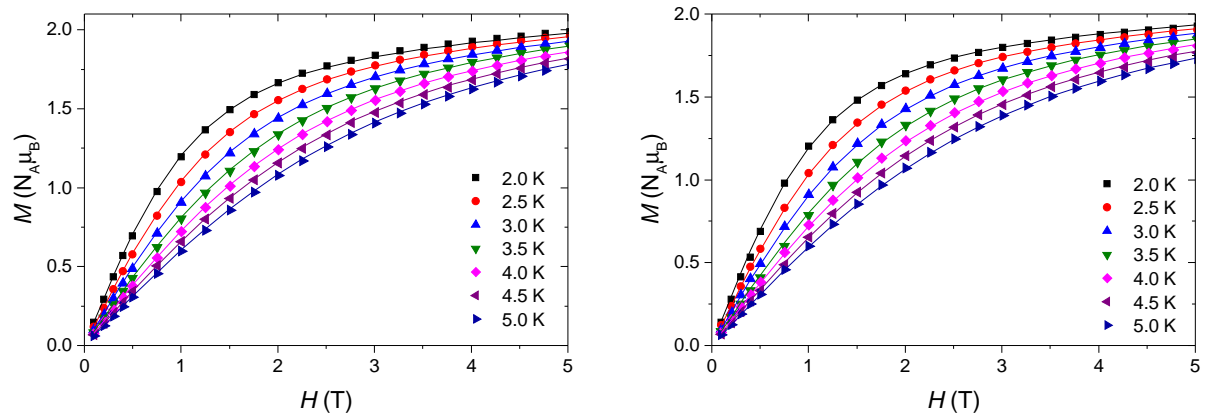


Fig. S5: Variable-field magnetization data at different temperatures of the complex **1** (left) and **2** (right). Lines represent simulation according to the parameters given in Table 3 in the manuscript.

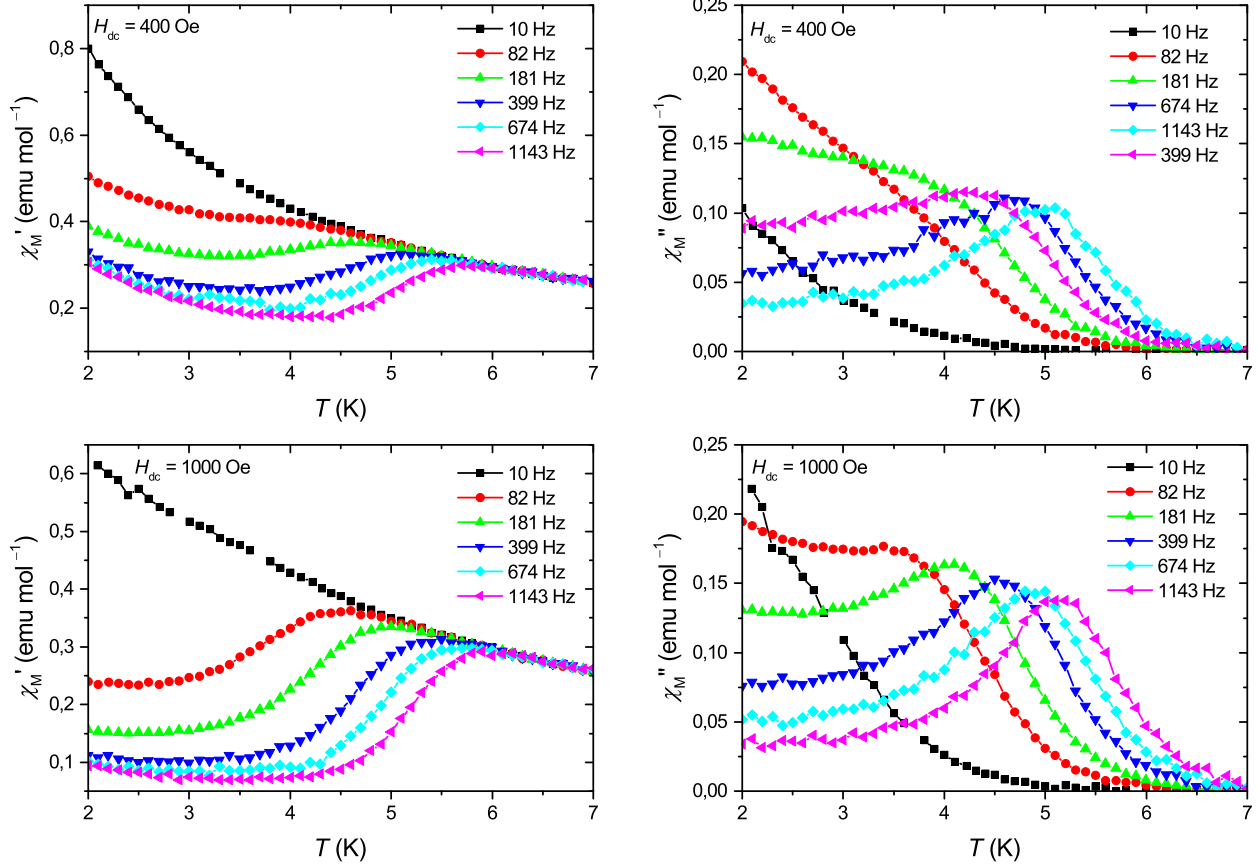


Fig. S6: Temperature dependence of the in-phase and out-of-phase ac susceptibility χ_M'' at different frequencies for **1**. Lines are guides for the eyes.

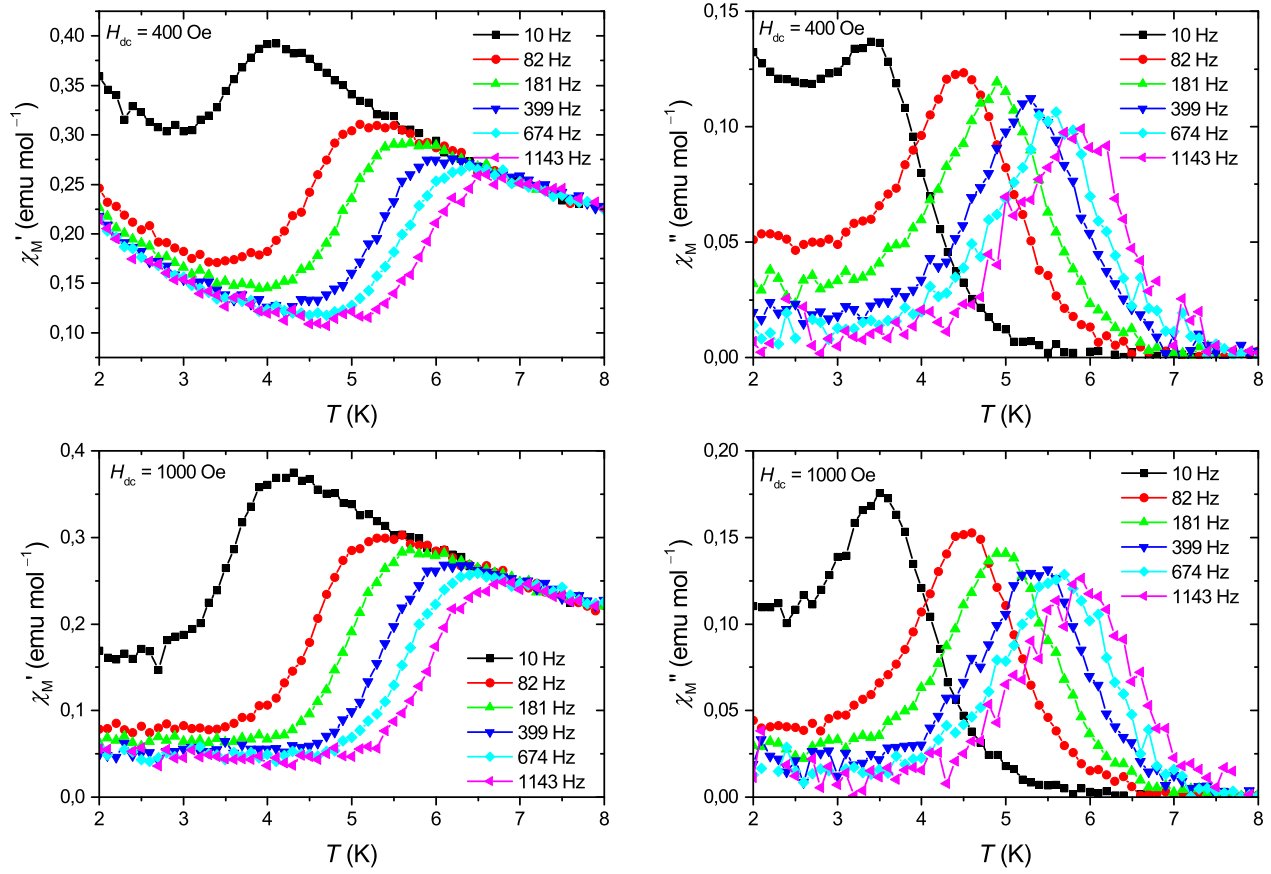


Fig. S7: Temperature dependence of the in-phase and out-of-phase ac susceptibility χ_M'' at different frequencies for **2**. Lines are guides for the eyes.

Table S3: Relaxation times τ_c and α parameters for the Cole-Cole fits of complex **1** with an applied field of 400 Oe

T (K)	τ_c (s)	α	χ_S (emu mol $^{-1}$)	χ_0 (emu mol $^{-1}$)
2.1	2.77×10^{-3}	0.149	0.278	0.804
2.2	2.58×10^{-3}	0.136	0.269	0.771
2.3	2.44×10^{-3}	0.135	0.258	0.739
2.4	2.28×10^{-3}	0.149	0.246	0.713
2.5	2.15×10^{-3}	0.146	0.233	0.682
2.6	1.98×10^{-3}	0.137	0.227	0.656
2.7	1.86×10^{-3}	0.133	0.222	0.632
2.8	1.77×10^{-3}	0.127	0.213	0.610
2.9	1.64×10^{-3}	0.126	0.206	0.590
3.0	1.55×10^{-3}	0.115	0.202	0.571
3.1	1.44×10^{-3}	0.133	0.194	0.556
3.2	1.31×10^{-3}	0.120	0.193	0.540
3.3	1.25×10^{-3}	0.110	0.188	0.522
3.4	1.17×10^{-3}	0.107	0.184	0.508
3.5	1.08×10^{-3}	0.104	0.179	0.495
3.6	9.85×10^{-4}	0.098	0.175	0.481
3.7	9.10×10^{-4}	0.076	0.173	0.466
3.8	8.58×10^{-4}	0.078	0.171	0.457
3.9	7.73×10^{-4}	0.071	0.165	0.446
4.0	6.90×10^{-4}	0.071	0.161	0.435
4.1	6.21×10^{-4}	0.065	0.156	0.425
4.2	5.51×10^{-4}	0.068	0.155	0.416
4.3	4.90×10^{-4}	0.051	0.153	0.405
4.4	4.37×10^{-4}	0.042	0.148	0.396
4.5	3.80×10^{-4}	0.047	0.147	0.391
4.6	3.42×10^{-4}	0.039	0.147	0.381
4.7	2.97×10^{-4}	0.033	0.140	0.372
4.8	2.49×10^{-4}	0.021	0.140	0.365
4.9	2.13×10^{-4}	0.001	0.150	0.358
5.0	1.95×10^{-4}	0.019	0.137	0.352
5.1	1.52×10^{-4}	0.014	0.139	0.345

Table S4: Relaxation times τ_c and α parameters for the Cole-Cole fits of complex **1** with an applied field of 1000 Oe

T (K)	τ_c (s)	α	χ_S (emu mol $^{-1}$)	χ_0 (emu mol $^{-1}$)
2.0	6.93×10^{-3}	0.254	0.054	0.858
2.1	6.56×10^{-3}	0.261	0.073	0.826
2.2	6.26×10^{-3}	0.264	0.069	0.800
2.3	5.47×10^{-3}	0.242	0.067	0.744
2.4	5.46×10^{-3}	0.259	0.066	0.734
2.5	5.09×10^{-3}	0.249	0.062	0.713
2.6	4.63×10^{-3}	0.250	0.062	0.682
2.7	4.34×10^{-3}	0.253	0.058	0.664
2.8	3.98×10^{-3}	0.232	0.055	0.635
2.9	3.67×10^{-3}	0.234	0.060	0.619
3.0	3.29×10^{-3}	0.219	0.054	0.594
3.1	2.98×10^{-3}	0.215	0.056	0.576
3.2	2.66×10^{-3}	0.187	0.054	0.552
3.3	2.40×10^{-3}	0.172	0.057	0.533
3.4	2.12×10^{-3}	0.167	0.060	0.518
3.5	1.88×10^{-3}	0.155	0.055	0.504
3.6	1.68×10^{-3}	0.137	0.057	0.487
3.7	1.49×10^{-3}	0.131	0.057	0.477
3.8	1.32×10^{-3}	0.110	0.056	0.461
3.9	1.16×10^{-3}	0.101	0.057	0.449
4.0	1.01×10^{-3}	0.086	0.058	0.436
4.1	8.76×10^{-4}	0.091	0.057	0.428
4.2	7.73×10^{-4}	0.067	0.055	0.415
4.3	6.55×10^{-4}	0.065	0.057	0.407
4.4	5.64×10^{-4}	0.052	0.053	0.397
4.5	4.92×10^{-4}	0.055	0.054	0.392
4.6	4.10×10^{-4}	0.040	0.054	0.380
4.7	3.47×10^{-4}	0.033	0.056	0.372
4.8	2.89×10^{-4}	0.032	0.055	0.365
4.9	2.44×10^{-4}	0.021	0.052	0.357
5.0	2.03×10^{-4}	0.015	0.055	0.351
5.1	1.66×10^{-4}	0.019	0.054	0.345
5.2	1.40×10^{-4}	0.010	0.053	0.338
5.3	1.13×10^{-4}	0.012	0.056	0.332

Table S5: Relaxation times τ_c and α parameters for the Cole-Cole fits of complex **2** with an applied field of 400 Oe

T (K)	τ_c (s)	α	χ_S (emu mol $^{-1}$)	χ_0 (emu mol $^{-1}$)
3.6	1.15×10^{-2}	0.219	0.128	0.510
3.7	9.17×10^{-3}	0.177	0.130	0.481
3.8	7.27×10^{-3}	0.162	0.124	0.462
3.9	6.04×10^{-3}	0.151	0.120	0.451
4.0	4.78×10^{-3}	0.109	0.119	0.430
4.1	4.14×10^{-3}	0.126	0.117	0.427
4.2	3.30×10^{-3}	0.091	0.116	0.406
4.3	2.72×10^{-3}	0.070	0.117	0.394
4.4	2.31×10^{-3}	0.076	0.114	0.392
4.5	2.04×10^{-3}	0.084	0.109	0.388
4.6	1.59×10^{-3}	0.067	0.106	0.375
4.7	1.33×10^{-3}	0.040	0.107	0.363
4.8	1.08×10^{-3}	0.054	0.104	0.357
4.9	9.00×10^{-4}	0.039	0.104	0.350
5.0	7.16×10^{-4}	0.082	0.094	0.347
5.1	6.13×10^{-4}	0.042	0.098	0.338
5.2	5.26×10^{-4}	0.032	0.098	0.329
5.3	4.29×10^{-4}	0.014	0.101	0.324
5.4	3.65×10^{-4}	0.020	0.097	0.319
5.5	3.06×10^{-4}	0.010	0.101	0.314
5.6	2.43×10^{-4}	0.008	0.098	0.309
5.7	2.20×10^{-4}	0	0.106	0.303
5.8	1.70×10^{-4}	0	0.099	0.299
5.9	1.42×10^{-4}	0.004	0.096	0.293
6.0	1.24×10^{-4}	0	0.111	0.290

Table S6: Relaxation times τ_c and α parameters for the Cole-Cole fits of complex **2** with an applied field of 1000 Oe

T (K)	τ_c (s)	α	χ_S (emu mol $^{-1}$)	χ_0 (emu mol $^{-1}$)
3.8	9.67×10^{-3}	0.153	0.045	0.471
3.9	7.80×10^{-3}	0.131	0.045	0.457
4.0	6.14×10^{-3}	0.113	0.044	0.437
4.1	4.98×10^{-3}	0.103	0.044	0.421
4.2	4.04×10^{-3}	0.102	0.041	0.412
4.3	3.35×10^{-3}	0.068	0.044	0.395
4.4	2.73×10^{-3}	0.058	0.043	0.384
4.5	2.38×10^{-3}	0.062	0.042	0.382
4.6	1.82×10^{-3}	0.050	0.040	0.367
4.7	1.52×10^{-3}	0.044	0.042	0.358
4.8	1.26×10^{-3}	0.054	0.038	0.354
4.9	1.02×10^{-3}	0.057	0.037	0.347
5.0	8.85×10^{-4}	0.036	0.046	0.340
5.1	6.93×10^{-4}	0.065	0.032	0.336
5.2	5.96×10^{-4}	0.023	0.038	0.325
5.3	4.94×10^{-4}	0.022	0.039	0.320
5.4	3.96×10^{-4}	0.027	0.039	0.314
5.5	3.20×10^{-4}	0.017	0.034	0.308
5.6	2.70×10^{-4}	0.031	0.033	0.306
5.7	2.50×10^{-4}	0	0.053	0.298
5.8	1.89×10^{-4}	0.012	0.041	0.295
5.9	1.59×10^{-4}	0	0.044	0.291
6.0	1.33×10^{-4}	0.015	0.047	0.284

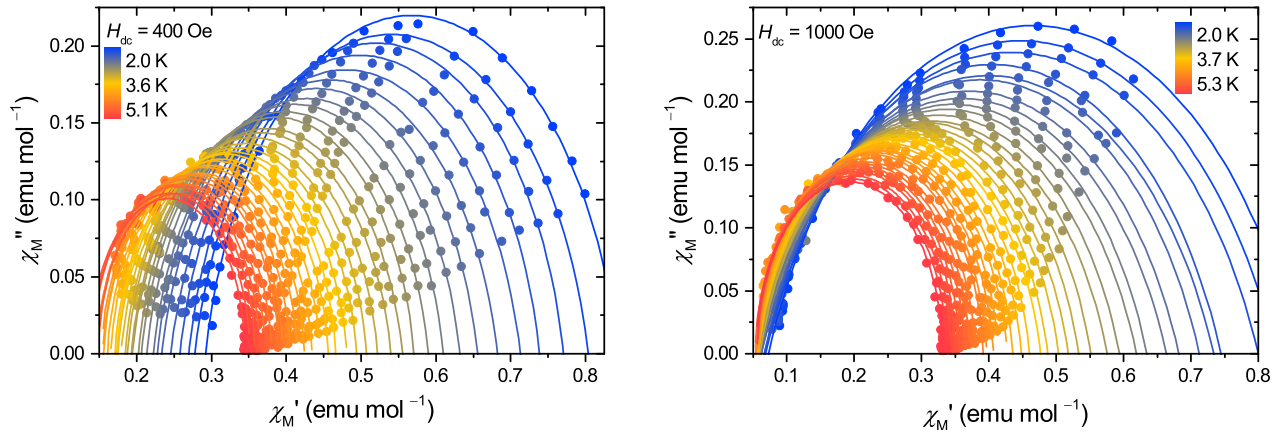


Fig. S8: Cole-Cole plots for complex 1 at different temperatures. Solid lines represent the best fit.

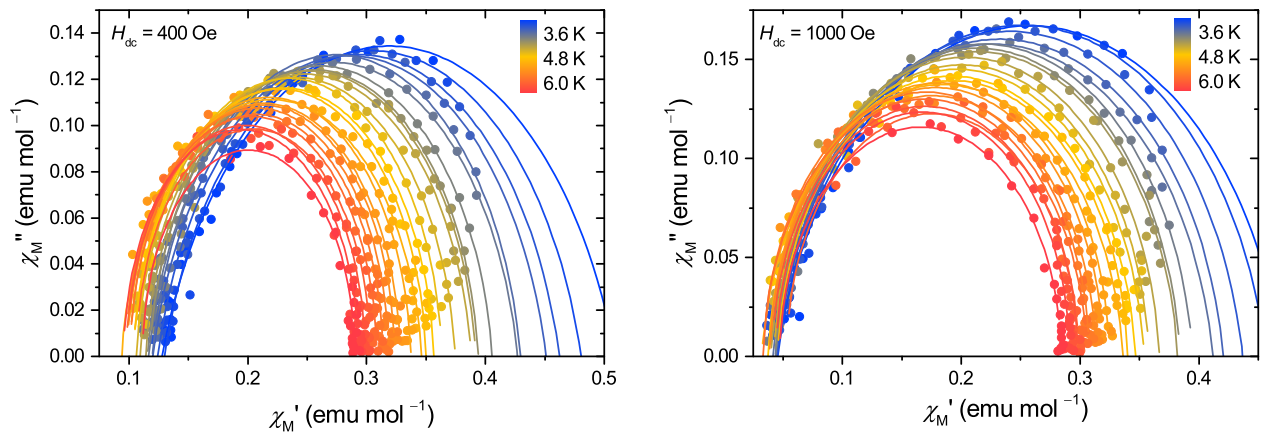


Fig. S9: Cole-Cole plots for complex 2 at different temperatures. Solid lines represent the best fit.

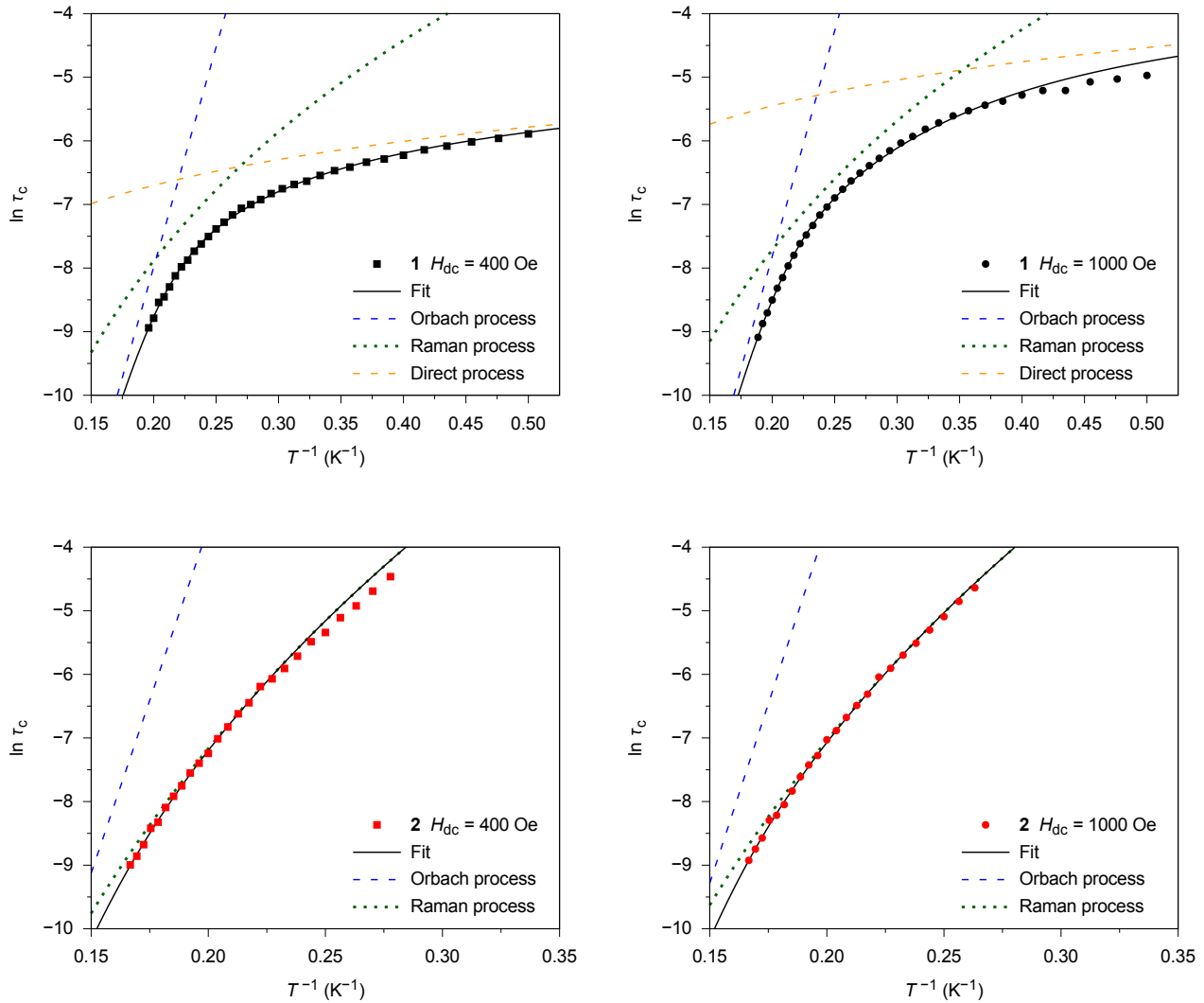


Fig. S10: Arrhenius plots of relaxation times for **1** (top row) and **2** (bottom row) with applied dc fields of 400 Oe (left column) and 1000 Oe (right column). The black line describes the best fit to Equation (3) with fixed n (**1**: $n = 5$; **2**: $n = 9$) and colored lines represent the contribution of specific relaxation processes (for parameters see Table 4).

Table S7: Parameters for the magnetic relaxation of complexes **1** and **2** obtained by fit of the relaxation times to Equation (3) with fixed n (**1**: $n = 5$; **2**: $n = 9$) and $U_{\text{eff}} = 2\sqrt{D^2 + 3E^2}$ (D and E are taken from FD-FT THz-EPR measurements, see Table 6)

	H_{dc} (Oe)	U_{eff} (cm^{-1})	τ_0 (s)	n	C ($\text{s}^{-1}\text{K}^{-n}$)	A ($\text{Oe}^{-4}\text{s}^{-1}\text{K}^{-1}$)
1	400	47.3	$4.1(1) \times 10^{-10}$	5.0	$8.4(4) \times 10^{-1}$	$6.4(3) \times 10^{-9}$
	1000	47.3	$4.68(5) \times 10^{-10}$	5.0	$6.6(1) \times 10^{-1}$	$5.2(4) \times 10^{-11}$
2	400	62.8	$1.6(2) \times 10^{-10}$	9.0	$6.3(2) \times 10^{-4}$	na
	1000	62.8	$1.4(1) \times 10^{-10}$	9.0	$5.4(2) \times 10^{-4}$	na

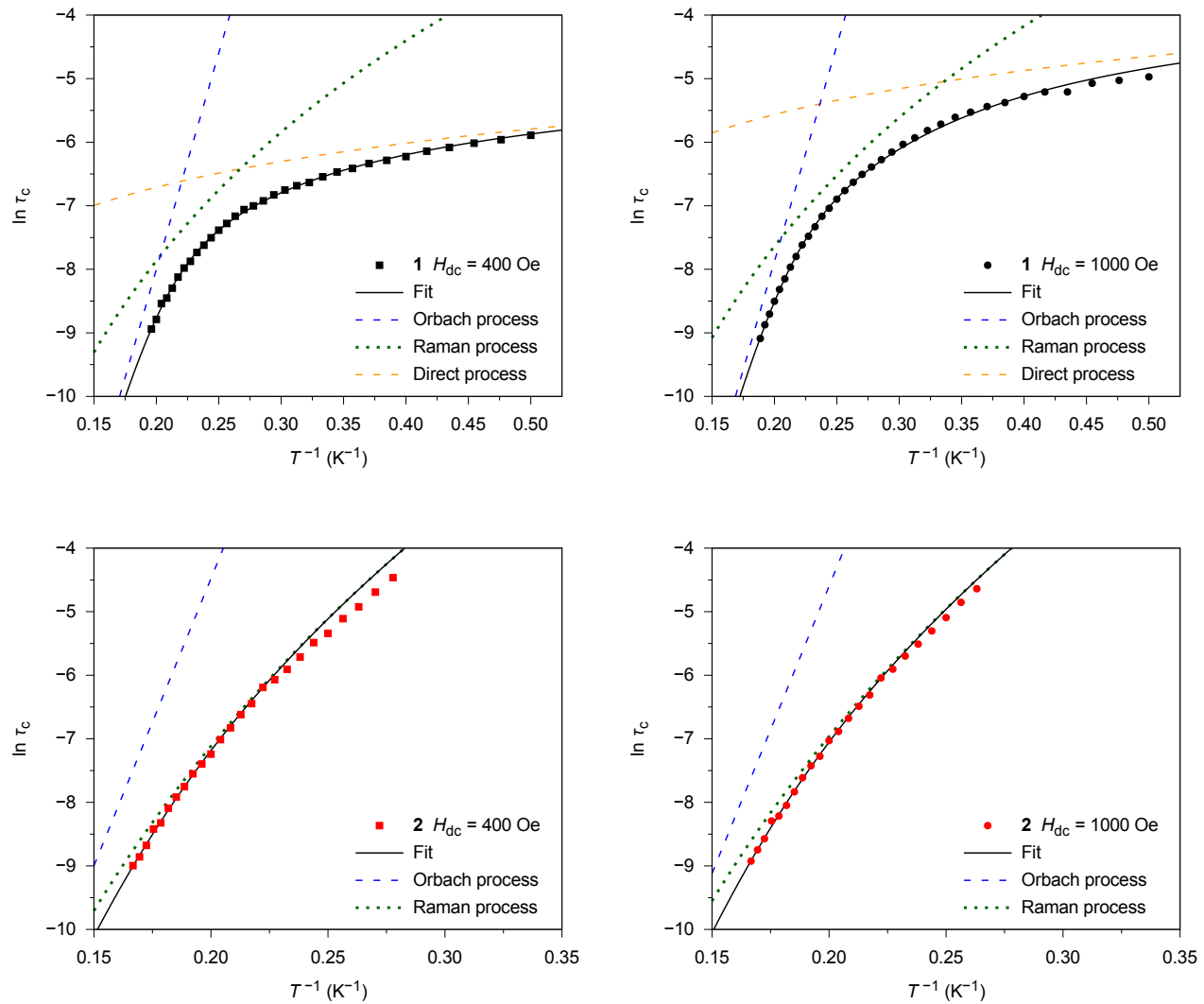


Fig. S11: Arrhenius plots of relaxation times for **1** (top row) and **2** (bottom row) with applied dc fields of 400 Oe (left column) and 1000 Oe (right column). The black line describes the best fit to Equation (3) with fixed n (**1**: $n = 5$; **2**: $n = 9$) and $U_{\text{eff}} = 2\sqrt{D^2 + 3E^2}$ (D and E are taken from FD-FT THz-EPR measurements, see Table 6) and colored lines represent the contribution of specific relaxation processes (for parameters see Table S7).

Table S8: Parameters obtained by fit of the Arrhenius plot by considering only the Orbach process

	H_{dc} (Oe)	U_{eff} (cm^{-1})	τ_0 (s)
1	400	22(1)	$2.4(9) \times 10^{-7}$
	1000	29.0(7)	$5(2) \times 10^{-8}$
2	400	35.7(7)	$2.6(4) \times 10^{-8}$
	1000	37.1(7)	$2.0(4) \times 10^{-8}$

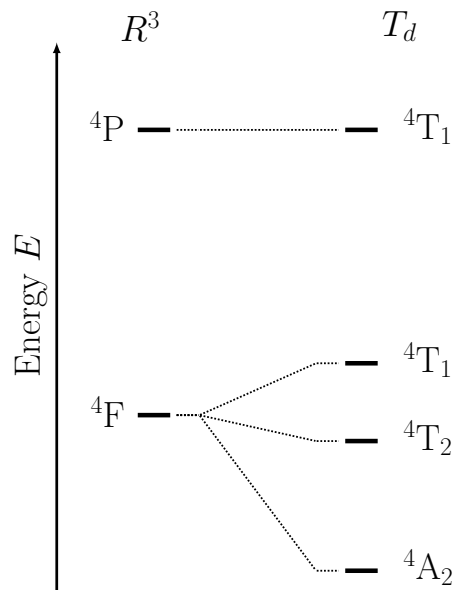


Fig. S12: Ligand-field splitting of a high-spin cobalt(II) ion in a (pseudo-)tetrahedral coordination environment.

Table S9: Relative CASSCF and CASPT2 energies (in cm^{-1}) for all quartet and the 12 lowest doublet states of **1** and **2**

$2S + 1$	Term	Subterm	1		2	
			CASSCF	CASPT2	CASSCF	CASPT2
4	^4F	$^4\text{A}_2$	0	0	0	0
		$^4\text{T}_2$	1865	2060	1612	1811
			4615	5304	4013	4642
			6297	6617	5675	6044
		$^4\text{T}_1$	8839	9951	8775	8143
	^4P		9112	9404	9254	9468
			9131	9107	9731	10900
		$^4\text{T}_1$	21779	19351	22249	20189
			22633	19496	22498	19422
			26256	23993	26833	24500
2	$^2\text{G} + ^2\text{P}$		16209	12837	15043	11664
			18115	15717	16691	14487
			18159	15206	17089	14161
			19391	16359	19108	16062
			19511	16127	19657	16236
			20642	17683	20706	17788
			21918	19170	21701	18985
			23361	20108	22937	19747
			24067	21976	23628	21541
			24542	22065	24366	22005
			25581	22949	25156	22613
			26070	22682	25904	22908

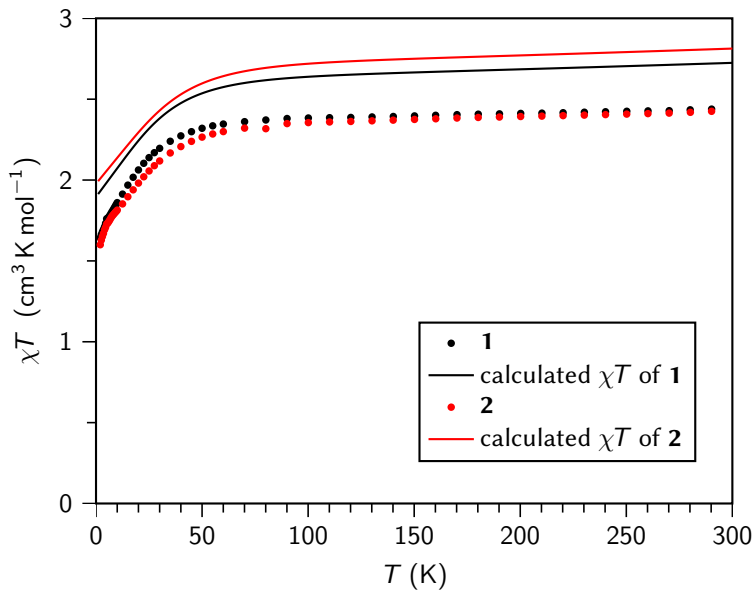


Fig. S13: Magnetic susceptibility χT for **1** (black line) and **2** (red line) as obtained with the SINGLE_ANISO module utilizing CASSCF/CASPT2/SO-RASSI wave functions.

Table S10: Relative SO-RASSI energies (in cm^{-1}) for the lowest Kramers doublets (KDs) of **1** and **2**

Term	KD	1	2
^4F	$^4\text{A}_2$	1	0
		2	73
$^4\text{T}_2$	3	1960	1721
	4	2113	1889
	5	4624	4035
	6	4773	4194
	7	6444	5863
	8	6534	5946
$^4\text{T}_1$	9	8654	8779
	10	8740	8818
	11	8974	9178
	12	9424	9558
	13	9584	10072
	14	9917	10289

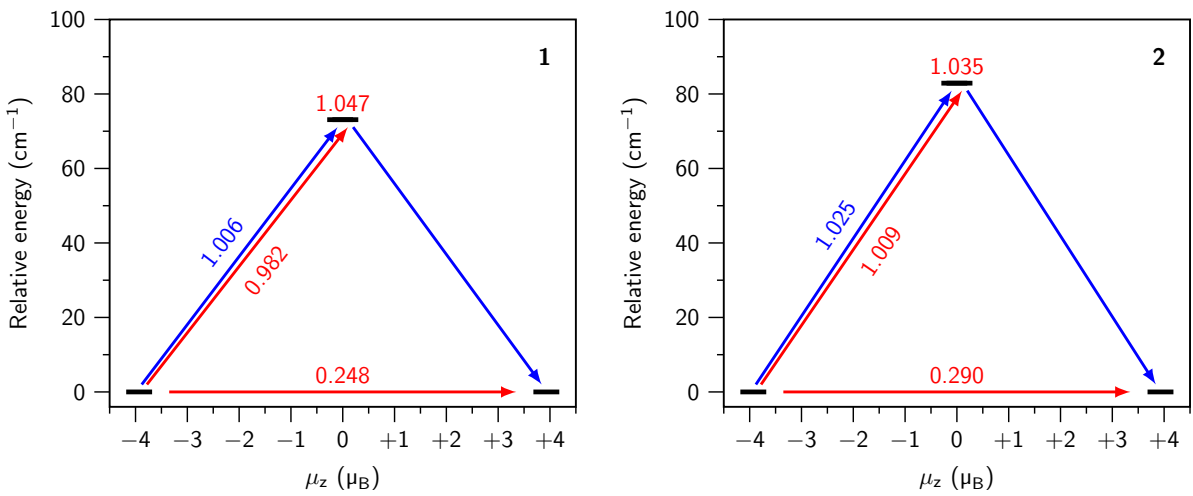


Fig. S14: Splitting of the two Kramers doublets of the $^4A_2[{}^4F]$ ground state for **1** (left) and **2** (right) in combination with their magnetic moments in the direction of the easy-axis. The arrows represent possible magnetic relaxation pathways between two states together with their average dipole transition matrix element as obtained by SINGLE_ANISO. Transitions marked in red represent an inversion of the sign of the magnetic moment, whereas blue represents the conservation of the sign. Only relaxation pathways from $|M_S = -3/2\rangle$ towards $|M_S = \pm 1/2\rangle$ and $|M_S = +3/2\rangle$ are shown.

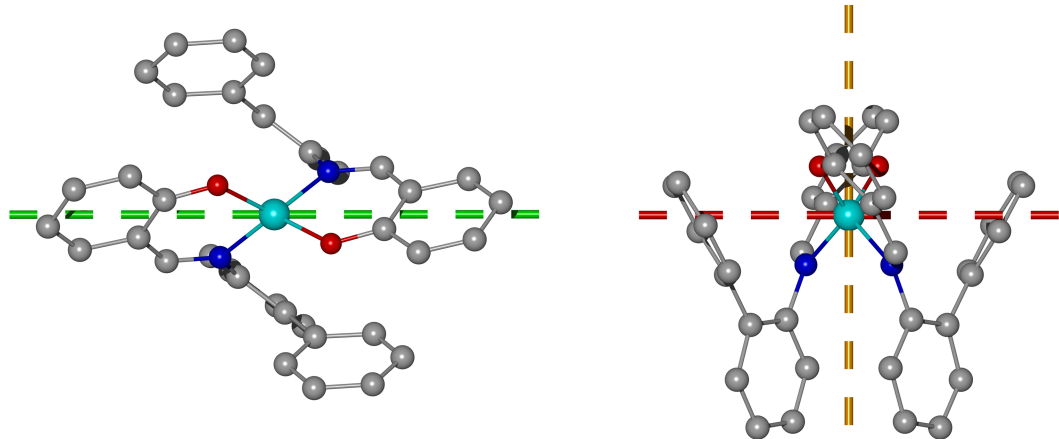


Fig. S15: *Ab initio* calculated magnetic axes ($S_{\text{eff}} = 3/2$; green dashed line: g_z ; yellow dashed line: g_y ; red dashed lines: g_x) for the ${}^4A_2[{}^4F]$ ground multiplet of **1**. Hydrogen atoms were omitted for clarity.

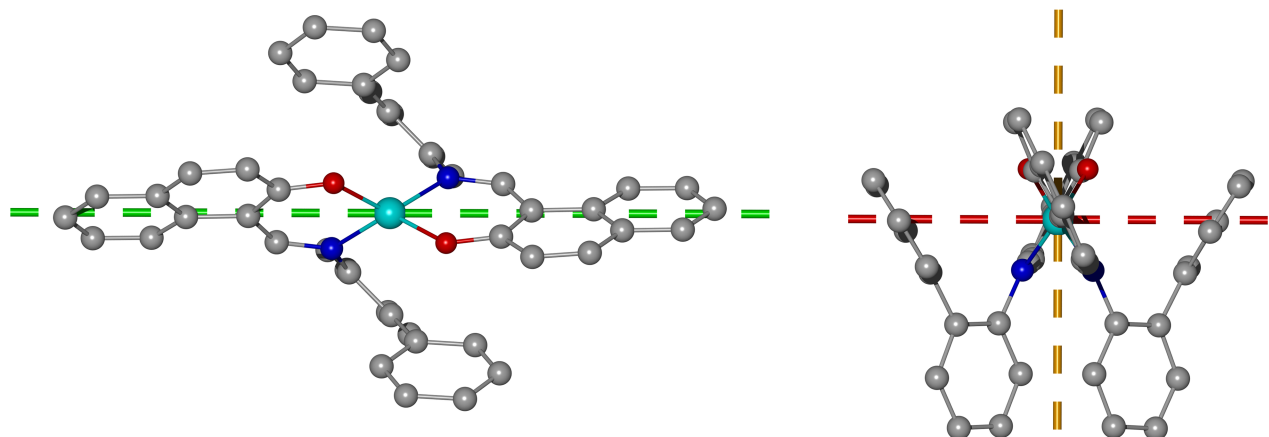


Fig. S16: *Ab initio* calculated magnetic axes ($S_{\text{eff}} = 3/2$; green dashed line: g_z ; yellow dashed line: g_y ; red dashed lines: g_x) for the ${}^4A_2[{}^4F]$ ground multiplet of **2**. Hydrogen atoms were omitted for clarity.

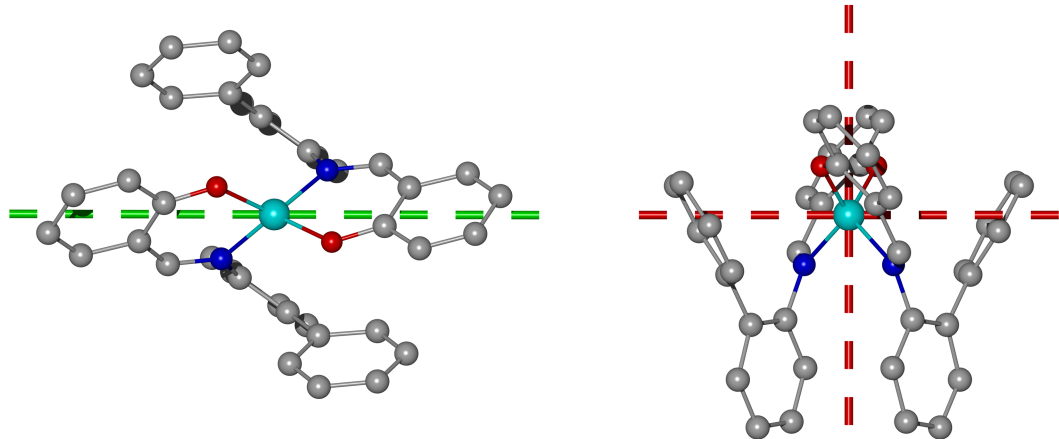


Fig. S17: *Ab initio* calculated magnetic axes ($S_{\text{eff}} = 1/2$; green dashed line: easy-axis; red dashed lines: hard-axes) for the ground state KD of **1**. Hydrogen atoms were omitted for clarity.

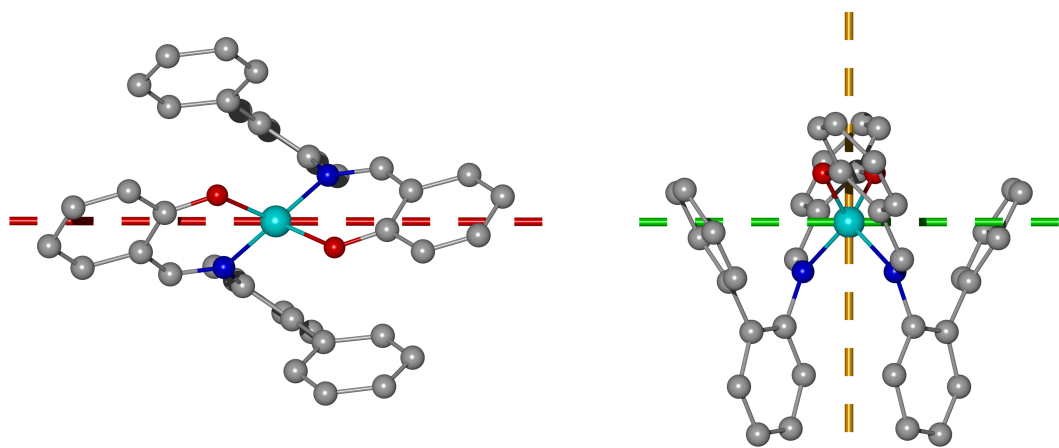


Fig. S18: *Ab initio* calculated magnetic axes ($S_{\text{eff}} = 1/2$; green dashed line: easy-axis; yellow dashed line: intermediate axis; red dashed line: hard-axis) for the first excited KD state of **1**. Hydrogen atoms were omitted for clarity.

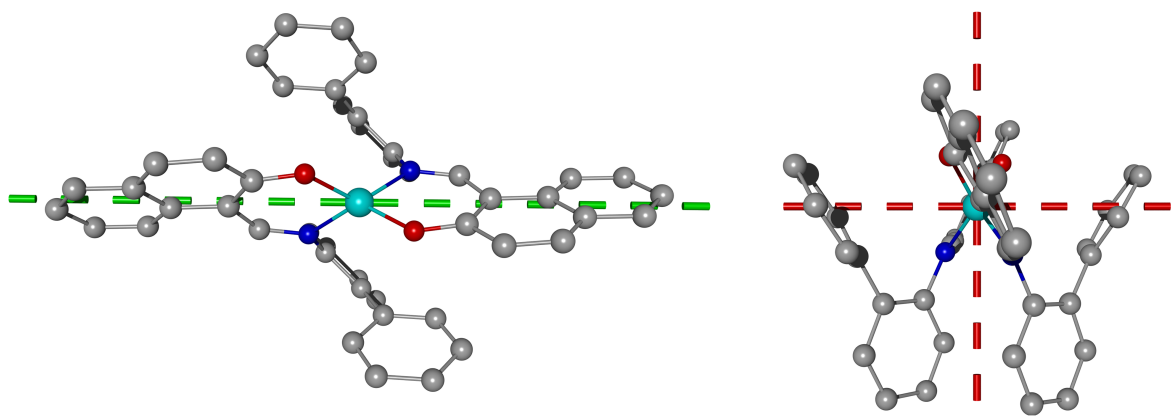


Fig. S19: *Ab initio* calculated magnetic axes ($S_{\text{eff}} = 1/2$; green dashed line: easy-axis; red dashed lines: hard-axes) for the ground state KD of **2**. Hydrogen atoms were omitted for clarity.

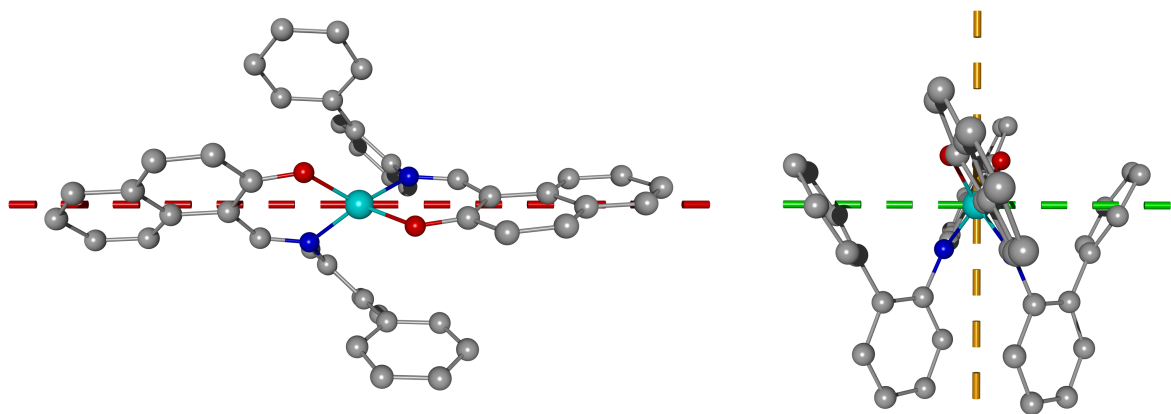


Fig. S20: *Ab initio* calculated magnetic axes ($S_{\text{eff}} = 1/2$; green dashed line: easy-axis; yellow dashed line: intermediate axis; red dashed line: hard-axis) for the first excited KD state of **2**. Hydrogen atoms were omitted for clarity.

Table S11: Relative SO-RASSI energies and their components of the g -tensor ($S_{\text{eff}} = 1/2$) for the two Kramers doublets (KDs) of the ${}^4\text{A}_2[{}^4\text{F}]$ ground state for **1** and **2**

		1	2
KD1	E_{KD1} (cm $^{-1}$)	0	0
	g_x	0.681	0.778
	g_y	0.807	0.960
	g_z	7.715	7.856
KD2	E_{KD2} (cm $^{-1}$)	73	83
	g_x	2.572	2.624
	g_y	3.640	3.539
	g_z	4.882	4.938

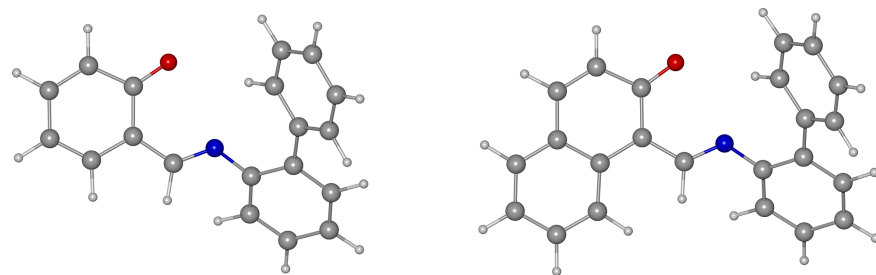


Fig. S21: Optimized structures of the deprotonated ligand species $(\text{L}^{\text{Sal},2\text{-Ph}})^-$ (left) and $(\text{L}^{\text{Nph},2\text{-Ph}})^-$ (right).

Table S12: Charges of the donor atoms for the deprotonated ligand species as obtained by population analyses (Mulliken and natural population analysis (NPA))

Ligand	Mulliken		NPA	
	O	N	O	N
$(\text{L}^{\text{Sal},2\text{-Ph}})^-$	-0.457	-0.203	-0.647	-0.451
$(\text{L}^{\text{Nph},2\text{-Ph}})^-$	-0.436	-0.215	-0.625	-0.446

Bibliography

- [S1] Cinčić, D.; Kaitner, B. Schiff base derived from 2-hydroxy-1-naphthaldehyde and liquid-assisted mechanochemical synthesis of its isostructural Cu(II) and Co(II) complexes. *CrysEngComm* **2011**, *13*, 4351–4357.